

CHEMISTRY

Affinity selection–mass spectrometry with linearizable macrocyclic peptide libraries

Michael A. Lee^{1†}, Joseph S. Brown^{1‡}, Charlotte E. Farquhar¹, Andrei Loas¹, Bradley L. Pentelute^{1,2,3,4*}

Despite their potential, the preparation of large synthetic macrocyclic libraries for ligand discovery and development has been limited. Here, we produce 100-million-membered macrocyclic libraries containing natural and non-natural amino acids. Near-quantitative intramolecular disulfide formation is facilitated by rapid oxidation with iodine in solution. After use in affinity selection, treatment with dithiothreitol enables near-quantitative reduction, rendering linear peptide analogs for standard tandem mass spectrometry. We use these libraries to discover macrocyclic binders to cadherin-2 and anti-hemagglutinin antibody clone 12ca5. Structure-activity relationship studies of an initial cadherin-binding peptide [CBP; apparent dissociation constant (K_d) = 53 nanomolar] reveal residues responsible for driving affinity (hotspots) and mutation-tolerant residues (coldspots). Two original macrocyclic libraries are prepared in which these hotspots and coldspots are derivatized with nonnatural amino acids. Following discovery and validation, high-affinity ligands are discovered from the coldspot library, with NCBP-4 demonstrating improved affinity (K_d = 29 nanomolar). Overall, we expect that this work will improve the use of macrocyclic libraries in therapeutic peptide development.

INTRODUCTION

Macrocyclic peptides show therapeutic promise with advantages over small molecules to disrupt protein-protein interactions and over proteins to cross biological membranes (1–4). Specifically, macrocyclization can impart several potential benefits to linear precursors, including increased proteolytic stability, cell permeability, binding affinity, and oral bioavailability (5, 6). Proteases often engage and degrade peptides in extended β -strand conformations (7, 8). Macrocyclization can offer proteolytic resistance by limiting conformational accessibility of the peptide backbone to the enzyme active site and enable the use of specific engineerable scaffolds (e.g., stapled α -helices) (9–12). Cyclization is central to the currently applied design principles to achieve passive cell permeability, in addition to strategies that modulate molecular weight, polar surface area, hydrogen bond interactions, and shape (13–16). Combining proteolytic stability and passive permeability can impart oral bioavailability for peptide-based drug candidates, which can further be improved by pharmaceutical formulation (17, 18). For these reasons, macrocyclic libraries are preferred for use with affinity selection-based peptide ligand discovery platforms. In addition, the direct identification of macrocyclic peptide binders from these selections streamlines subsequent development by alleviating the need to optimize suitable cyclization sites. Last, the conformational constraint imparted by macrocyclization may improve discovery rates of ligands from libraries against challenging targets (19–21).

Genetically encoded discovery platforms generally access macrocyclic peptide libraries while focusing on high diversity ($>10^8$ members) (22–28), while synthetic libraries can access the nonnatural chemical space at lower diversity ($<10^8$ members) (29–33). While

more stable macrocyclization linkages are preferred (24, 34), the disulfide linkage is suitable at the ligand discovery stage and does not require any chemical modification or treatment that could compromise genetic amplification in some platforms (28, 35). The disulfide linkage has been used to create macrocyclic libraries for over two decades in phage display discovery platforms (36–38) and is commonly encountered in clinically approved drugs (5, 39). Such drugs include vasopressin analogs as used to treat diabetes insipidus, somatostatin analogs like octreotide and lanreotide as used to treat carcinoid syndrome and gastrointestinal disorders (40, 41), and calcitonin as used to regulate calcium levels and to treat osteoporosis (42).

While the disulfide bond is present in many clinically approved drugs, it is also common for the disulfide linkage to be replaced during lead optimization. Many strategies have been used to replace the disulfide bond, including thioether linkages (43–46), amide linkages (47–50), carba bridges (51, 52), diselenide bonds (53–55), or triazole bridges (56, 57). These methods have been explored for peptide ligands and hormones and serve as models for handling disulfide replacement for further development of drug candidates. From a disulfide starting point, replacement is a typical early part of development and has been documented to potentially affect the secondary structure of the peptide and engagement with a given target. Thus, depending on the manner of target engagement, the replacement of the disulfide with a more stable analog can result in positive (48), negative (45–47, 52, 58), or minimal effect (43, 44, 49, 56) on function relative to the original peptide. Thus, replacement of the disulfide is often investigated early in hit-to-lead optimization to recover and improve upon the occasional decrease in potency. Nevertheless, few are as facile to chemically use and reverse as the disulfide, suggesting their potential use in large synthetic libraries.

Synthetic libraries generally leverage the broader use of nonnatural or abiotic functionalities, which have frequently appeared critical to the success of clinical peptide drug candidates including inhibitors to the interleukin-23 receptor, mouse double minute 2, β -catenin, and proprotein convertase subtilisin/kexin type 9 (17, 29, 59–61). Using disulfide macrocyclization for synthetic libraries leverages a highly efficient and easily implemented method for cyclization, as no additional

Copyright © 2025 The Authors, some rights reserved; exclusive licensee American Association for the Advancement of Science. No claim to original U.S. Government Works. Distributed under a Creative Commons Attribution NonCommercial License 4.0 (CC BY-NC).

¹Department of Chemistry, Massachusetts Institute of Technology, Cambridge, MA 02139, USA. ²The Koch Institute for Integrative Cancer Research, Massachusetts Institute of Technology, Cambridge, MA 02142, USA. ³Center for Environmental Health Sciences, Massachusetts Institute of Technology, Cambridge, MA 02139, USA. ⁴Broad Institute of MIT and Harvard, Cambridge, MA 02142, USA.

*Corresponding author. Email: blp@mit.edu

†These authors contributed equally to this work.

‡Present address: Acceleration Consortium, University of Toronto, Toronto, ON M5G 1Z5, Canada.

purification steps are required compared to a linear library. Because they cannot be genetically encoded or amplified, synthetic libraries are screened directly (30) as in affinity selection decoded by mass spectrometry (AS-MS) (62–64). With a key exception of DNA-encoded libraries (65), state-of-the-art synthetic macrocyclic libraries generally number below tens of thousands of individual compounds (30), compared to the high-diversity libraries (10^8 members) used in this work.

The complexity of decoding macrocyclic peptide sequences in mass spectrometry (MS) is a historic limitation for the use of synthetic macrocyclic libraries in affinity selection discovery platforms. Experimental approaches for decoding macrocyclic libraries include computational processing of mass spectra (66–69) and chemically triggered linearization (64, 70–75). Computational approaches process primary, secondary, and various tertiary mass spectra of cyclic peptide fragments and have excelled where database matching is possible (66, 69). For de novo sequencing, the complexity of enumerating virtual spectra markedly increases as the number of monomers and library size increases and has only been demonstrated up to ~1000-membered libraries (67, 76). Chemically triggered linearization adds a synthetic step that must be near quantitative and high yielding to enable bottom-up sequencing of noncyclic peptides, which has been demonstrated at very high diversities (77). However, most chemical linearization treatments are harsh and/or rely on the inclusion of nonstandard chemical functional groups at fixed positions, limiting library composition (64, 70–75). Cyclization techniques using either of the termini have inherent limitations on structural diversity, whereas side chain to side chain cyclization potentially alleviates these limitations. Moreover, these approaches have yet to be demonstrated on high-diversity libraries (~ 10^8 members or more). Genetically encoded techniques, such as mRNA display, can use more stable macrocyclization strategies due to sequencing not relying on the peptide structure but rather an accompanying RNA strand (24, 34). However, synthetic peptide libraries allow for facile incorporation of any number of unnatural amino acids, notably in the case where several consecutive unnatural residues are desired (78). While mRNA display approaches are expanding in scope of unnatural amino acid incorporation, the ample access allotted by synthetic libraries enables a wider exploration of the potential ligand space.

We demonstrate here ligand discovery from high-diversity libraries (10^8 members) using AS-MS against anti-hemagglutinin antibody clone 12ca5 (hereinafter abbreviated as 12ca5) and mouse cadherin-2 (CDH2). Cyclization by disulfide bond formation is accomplished using aqueous iodine. We verify the integrity of the library using Ellman's

assay and size exclusion chromatography (SEC) to confirm near-quantitative intramolecular macrocyclization of synthetic combinatorial libraries. Linearization is accomplished by mild reduction with heat and 1,3-dithiothreitol (DTT) and confirmed by Ellman's assay to enable standard tandem MS (MS/MS) sequencing. We apply these macrocyclic high-diversity libraries containing natural and nonnatural (or non-canonical) amino acids in an MS-based affinity selection platform for de novo peptide ligand discovery.

We demonstrate successful discovery of nanomolar ligands against 12ca5 and the ectodomain of CDH2. The 12ca5 protein binds peptides containing the sequence D**DY(A/S) (79, 80). While 12ca5 has been used to benchmark linear AS-MS libraries (33, 81), we use it here to benchmark and additionally validate the use of the high-diversity macrocyclic libraries. CDH2 was considered as a second target because of the potential impacts for chemical biology that an affinity reagent could provide, ranging from basic cell adhesion, to neural synapses formation (82), to the construction of intercalated discs of mammalian heart (83), as well as potential drug delivery due to its relative tissue selectivity in the brain and heart (84). These critical roles in biology are generally facilitated by homodimerization in domains 1 and 2 (82, 85, 86). Thus, we sought to discover ligands that bind to CDH2 domains 4 and 5 as they may not interfere with cadherin-2 function. Outside of domains 1 and 2, there are no ligands to CDH2 to our knowledge (85, 86). Last, we demonstrate the incorporation of nonnatural amino acids for second-generation ligand discovery in libraries designed with input gained by structure-activity relationship (SAR) data gathered on the initially discovered cadherin-binding peptide (CBP; Fig. 1). Together, the successful discovery of macrocyclic ligands to both targets from AS-MS demonstrates the potential deployment of ultra-large synthetically prepared macrocyclic libraries for peptide ligand discovery and development.

RESULTS

Because of its demonstrated utility in genetically encoded libraries, disulfide-induced macrocyclization of peptides has become a routine approach with a variety of existing methods to facilitate the oxidation step. Several different methods exist to form the disulfide linkage on single peptides, including oxidation using dimethyl sulfoxide (87), a gentle stream of air, or aqueous iodine with ≤5% methanol. Ideally, the macrocyclization step can be introduced during standard peptide library synthesis without incurring production

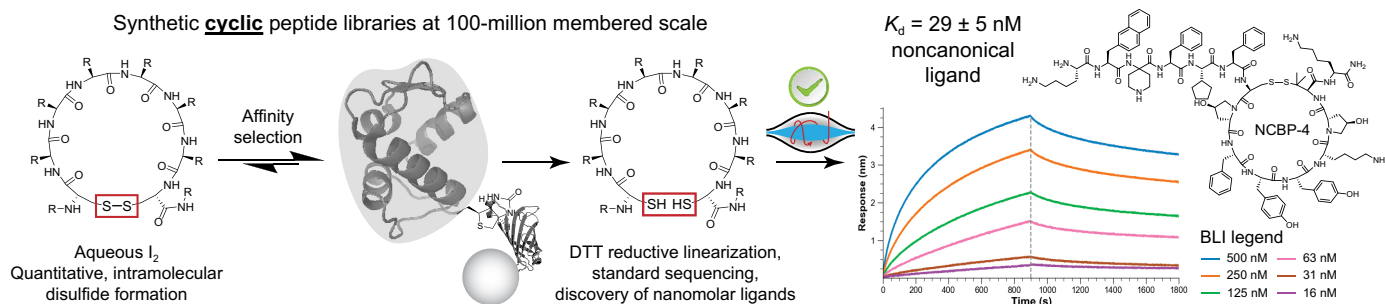


Fig. 1. Disulfide linkages allow for high-number diversity libraries compatible with decoding by MS/MS. Libraries of macrocyclic peptides are prepared for affinity selection by oxidation of cysteine analogs using aqueous iodine, providing a near-quantitative conversion to intramolecular macrocyclic peptides. Affinity selection facilitates the isolation of high-affinity ligands to a protein of interest. After affinity selection, peptides can be quickly linearized using DTT and standard de novo liquid chromatography (LC)-tandem MS (MS/MS) sequencing methods can be applied due to the linearization step. Ligand affinity is confirmed by a biophysical assay [i.e., bio-layer interferometry (BLI)].

delays or yield losses. The isolation of peptides in dimethyl sulfoxide (DMSO)-containing solutions could be challenging as the solvent cannot be easily evaporated or lyophilized and solid-phase extraction (SPE) could incur sample loss due to the DMSO content without further aqueous dilution (88). In comparison, oxidation using iodine presents itself as a rapid method compatible with mixtures of aqueous or organic solvents and can even facilitate the formation of disulfide bonds on resin during solid-phase peptide synthesis (62, 89). However, longer reaction times on resin promote iodine-based side reactions; therefore, rapid in-solution oxidation is preferred (<15 min) (89).

Iodine facilitated formation of macrocyclic peptide libraries at 100-million-membered scale (Fig. 2). We synthesized macrocyclic libraries by split-and-pool solid-phase peptide synthesis using mono-sized 20- μ m resin (8.33 g of resin, 2.00-mmol scale total), with each bead providing ~ 1 pmol of peptide. Two billion-membered libraries were prepared with the designs of CX_{12}CK and $\text{X}_6\text{CX}_6\text{CK}$, where X = all canonical amino acids except Cys, to control disulfide formation, and Ile because it is isobaric in mass with Leu (18 amino acids) and C = cysteine, homocysteine, and penicillamine (Fig. 3A). The libraries were split into five separate 100-million-membered aliquots and cleaved from the solid phase resin using a cleavage cocktail. After ether trituration and lyophilization, peptide libraries were cyclized in 5% acetonitrile in water (with 0.1% trifluoroacetic acid) at ~ 2 mg/ml (~ 1 mM) by dropwise addition of ~ 1 equiv. iodine in methanol until a yellow-brown color persisted. After 5 to 10 min at room temperature in the dark, the reaction was quenched with aqueous ascorbic acid to provide a colorless solution again (3.5 equiv.). Following solid-phase extraction, these libraries were then characterized to verify the efficiency of the oxidation and linearization reactions as well as their structure (intramolecular versus intermolecular disulfide formation).

Iodine-promoted cyclization was highly efficient and provided near-quantitative oxidation to disulfide by thiol quantification using Ellman's assay. We quantitated thiol oxidation by performing an Ellman's assay, normalized by the absorbance of the library at 280 nm

(Fig. 2A). The thiol content of the library was quantified by Ellman's reagent after cleavage, cold ether trituration, and SPE, to remove any remaining reducing scavengers. Upon aqueous resuspension of the library, a strong thiol signal was observed. This signal was eliminated completely by the treatment of the library with iodine, ascorbic acid quench, SPE purification, and aqueous resuspension, consistent with the near-quantitative formation of disulfide bonds.

With macrocyclic libraries in hand, a MS-friendly protocol to reduce and linearize the peptides was devised to enable standard tandem sequencing approaches. Both DL-DTT and immobilized tris(2-carboxyethyl)phosphine (TCEP) were considered for disulfide reduction. For experimental ease, TCEP was used in a bead-immobilized form, whereas DTT was directly added to each sample just before MS, reducing handling steps and potential sample loss. Because of its high solubility, DTT was used at 50 mg/ml, (~ 1000 equiv.) at 60°C for 15 min, whereas immobilized TCEP was used at 20 equiv. at room temperature for 25 min per the manufacturer's protocol (90). For DTT-treated samples, an SPE purification was performed to remove excess DTT reagent, whereas samples treated with immobilized TCEP were isolated by centrifugation. While TCEP only provided incomplete reduction (40% for $\text{X}_6\text{CX}_6\text{CK}$ and 85% for CX_{12}CK), DTT provided near-quantitative disulfide reduction ($\sim 100\%$ of original Ellman's signal across all libraries; fig. S1). Additionally, the reduction efficiency by DTT was found to be similar at pH 3 and pH 8 (fig. S1). The direct reduction at pH 3 was performed to mimic a prepared sample in 0.1% formic acid in water, which could then directly be injected in the mass spectrometer for tandem sequencing. Overall, these data support the near-quantitative formation and reduction of disulfide bonds.

SEC confirmed the disulfide bonds formed correspond to intramolecular species, producing an almost-exclusively monomeric macrocyclic peptide library. Using SEC to separate the library by its apparent molecular weight, we assessed whether the iodine-facilitated disulfide bond formation was intramolecular or intermolecular. Library samples were injected on a SuperDex 30 10/300 GL column,

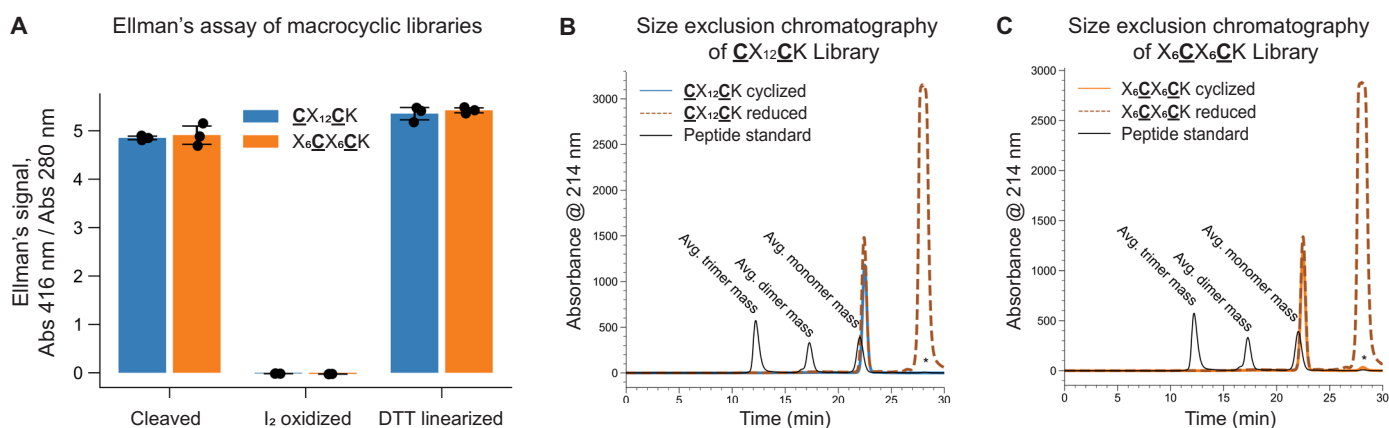


Fig. 2. Characterization of macrocyclic libraries based on size and thiol concentration showed near-quantitative formation of intramolecular disulfide bonds.

(A) Ellman's assay showed expected changes in total thiol concentration of the peptides directly after cleavage from the solid phase resin, after oxidation by dropwise addition of ~ 1 equiv. of 60 mM iodine in methanol to facilitate disulfide formation (room temperature, 5 to 10 min in the dark, subsequent quench with 3.5 equiv. aqueous ascorbic acid), and after reduction using DTT (50 mg/ml, ~ 1000 equiv. at 60°C for 15 min). Free thiol was quantitatively consumed during the oxidation process and was restored after linearization to concentrations comparable to those determined directly after cleavage. (B and C) Size exclusion chromatograms of absorbance at 214 nm of two macrocyclic libraries compared to molecular weight standards corresponding to the average mass of monomeric, dimeric, and trimeric species. Library samples were run using the cyclized form (later used in affinity selection experiments) and the DTT linearized form, demonstrating the formation of intramolecular disulfide bonds. Peaks marked with an asterisk (*) were residual elements from the sample buffer. C = cysteine, homocysteine, and penicillamine.

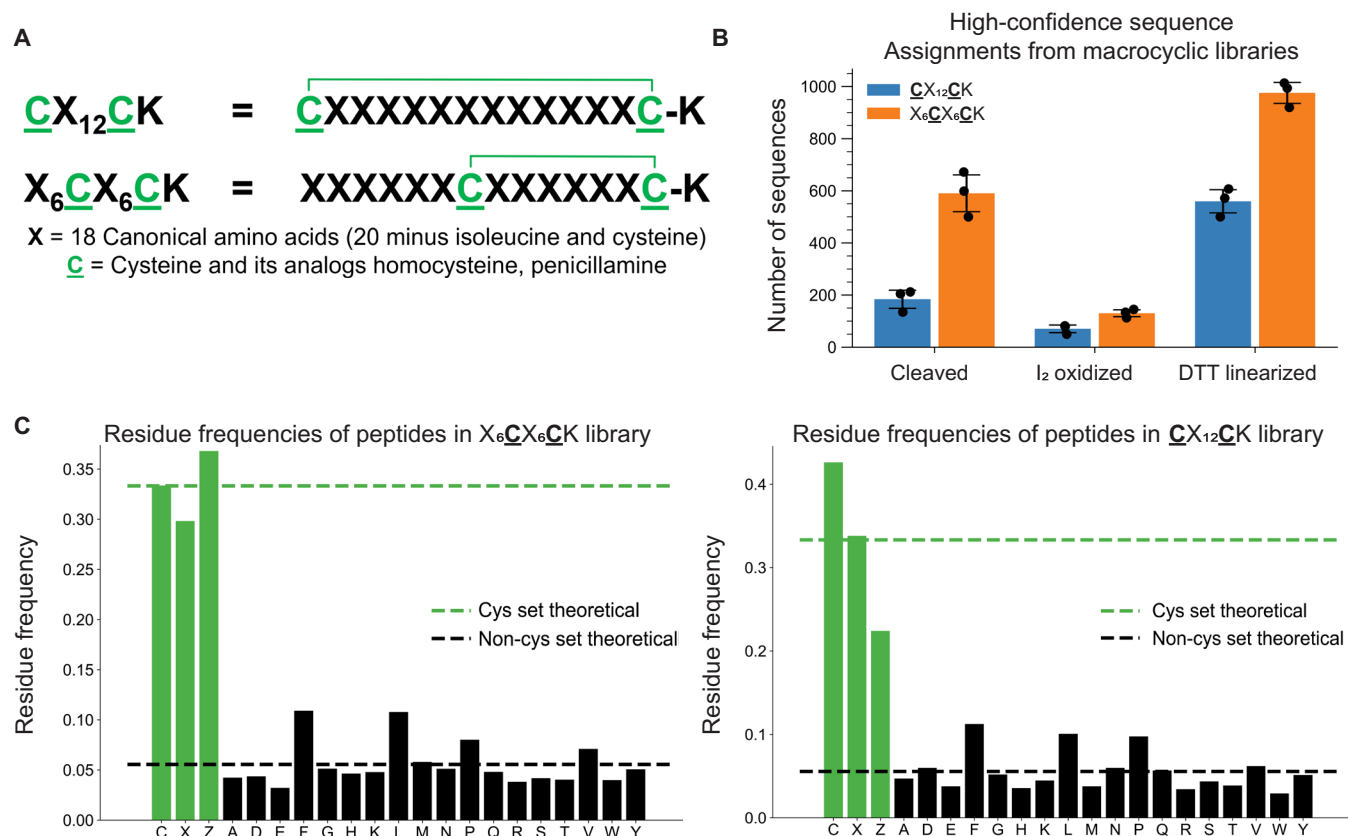


Fig. 3. Characterization of the macrocyclic peptide libraries by MS/MS sequencing shows successful split-and-pool synthesis of 15-residue libraries. (A) The macrocyclic peptide libraries were synthesized according to two designs, with a large 12-membered macrocycle or a smaller 6-membered macrocycle. Additionally, cysteine analogs including homocysteine and penicillamine were used to increase the diversity around the resulting disulfide linkage. (B) High-confidence sequence assignments of ~1000-membered library samples directly after cleavage, after oxidation by I₂, and after subsequent reduction using DTT show a loss and gain of sequencing capabilities with the macrocyclization process as expected ($n = 3$). High-confidence sequences were determined as having a calculated average local confidences for the de novo sequence assignment by PEAKS Studio 8.5 greater than 85% and an absolute mass error < 5 parts per million. (C) Normalized residue frequencies assignments (as a fraction) show a balanced incorporation of amino acids in the variable positions (black) and cysteine analog positions (green; X is homocysteine, and Z is penicillamine).

which can distinguish the molecular weight range of 100 to 7000 Da, to analyze the presence of monomeric, dimeric, and oligomeric peptides induced by iodine oxidation. Aliquots of 25 μg of library were injected after oxidation by iodine and purification by SPE, as well as in the reduced form after treatment with DTT. A custom low-molecular weight peptide standard was also prepared using peptides that correspond to the average molecular weights of monomeric, dimeric, and trimeric species along with the exclusion limit of the column; the components of the custom standard are given in table S1. As shown in Fig. 2 (B and C), only monomeric library species were observed when compared to the peptide standard, indicating that the disulfide bonds formed were intramolecular rather than intermolecular. This result, in tandem with the data from the Ellman's assay, asserted a nearly quantitative conversion of peptide thiols to intramolecular disulfide bonds and confirmed this technique provides a facile method for preparing high-diversity macrocyclic peptide libraries.

The high-diversity macrocyclic libraries are compatible with standard MS/MS sequencing protocols, and DTT facilitated the expected recovery of high-confidence peptide sequencing. Small aliquots of library (~1000 beads equivalent to ~1000 sequences) were taken at various points in the affinity selection workflow from cyclization to

linearization, including directly after cleavage from resin, after cyclization with iodine, and after linearization with DTT. About 8 μg of peptide library was purified via a C₁₈ StageTip (91) from three steps in the protocol: linear from cleavage, iodine macrocyclized, and DTT linearized. As expected, the library samples taken directly after cleavage and after linearization showed high sequencing confidence, described by de novo sequence IDs using PEAKS Studio 8.5 with an assigned local confidence greater than 85% and an absolute mass error < 5 parts per million (see Fig. 3B and fig. S2) (92). Conversely, the macrocyclized library sample showed poor sequencing confidence, consistent with unproductive fragmentation caused by the disulfide macrocycle. Last, the linearization by DTT in the MS sample provided a substantial recovery of the peptides discovered in standard tandem sequencing methods (Fig. 3B).

Analysis of the MS/MS sequencing data demonstrated a balanced distribution of amino acid monomers throughout the library, as well as the incorporation of noncanonical cysteine analogs. Histograms showing the monomer distribution among high-confidence sequence assignments are given in Fig. 3C. Although penicillamine and methionine are isobaric, the fixed positions of penicillamine allowed for effective filtering of sequences to prevent inaccurate assignments. The

X_6CX_6CK library design sequenced with higher confidence overall compared to the $CX_{12}CK$ library design, suggesting a benefit of the intermediate cysteine position during fragmentation events in sequence assignment. Overall, these results corroborate the successful split-and-pool synthesis, oxidation, reduction, and tandem sequencing decoding of the macrocyclic libraries.

Macrocyclic low-nanomolar peptide ligands were discovered by AS-MS performed against 12ca5 as a model protein target. The anti-hemagglutinin protein 12ca5 binds peptides containing the sequence D**DY(A/S) and has been used to benchmark AS-MS libraries (33, 79–81). Seven high-affinity peptide ligands were pulled down from the X_6CX_6CK library design, while only one peptide was from the $CX_{12}CK$ library (see table S2 for all identified sequences). A select number of these sequences were synthesized and validated (see fig. S3) for their binding affinity using biolayer interferometry (BLI). All identified binders exhibited apparent dissociation constants (K_d) in the low-nanomolar to high-picomolar range, nearing the lower limit of detection for the instrument (see Fig. 4 and fig. S4). The binding motif was present in the same position or frameshift in all sequences found from the X_6CX_6CK library. Specifically, the cysteine analog in the middle of the library design was located inside of

the 12ca5 motif at the third position [i.e., D* Ψ DY(A/S), where Ψ was discovered to be cysteine, homocysteine, or penicillamine].

Nanomolar affinity binders to CDH2 were discovered by AS-MS with the macrocyclic libraries. Due to the critical roles of CDH2 in adhesion in neural and cardiac junctions, the discovery of ligands outside of the protein homodimerization site could be of importance toward its study without affecting biological function. The homodimerization of CDH2 is largely driven by molecular interactions involving domains 1 and 2 of the ectodomain (82, 83, 85, 86). On the basis of these considerations, a fusion protein construct comprising domains 4 and 5 of the CDH2 ectodomain (residues 498 to 724; UniProt, P15116) was used as the target for AS-MS selections. The fusion protein was cloned and expressed in mammalian cells; purified using SEC and anti-protein C (clone HPC4) affinity tag purification; and verified by analytical SEC, reducing and nonreducing SDS–polyacrylamide gel electrophoresis gels, as well as Western blotting (fig. S5). To our knowledge, no peptide or small molecule ligands have been reported to these CDH2 domains outside the homodimerization site (85, 86).

Nanomolar peptide ligands were discovered by AS-MS with both X_6CX_6CK and $CX_{12}CK$ libraries against the CDH2[498-724] fusion

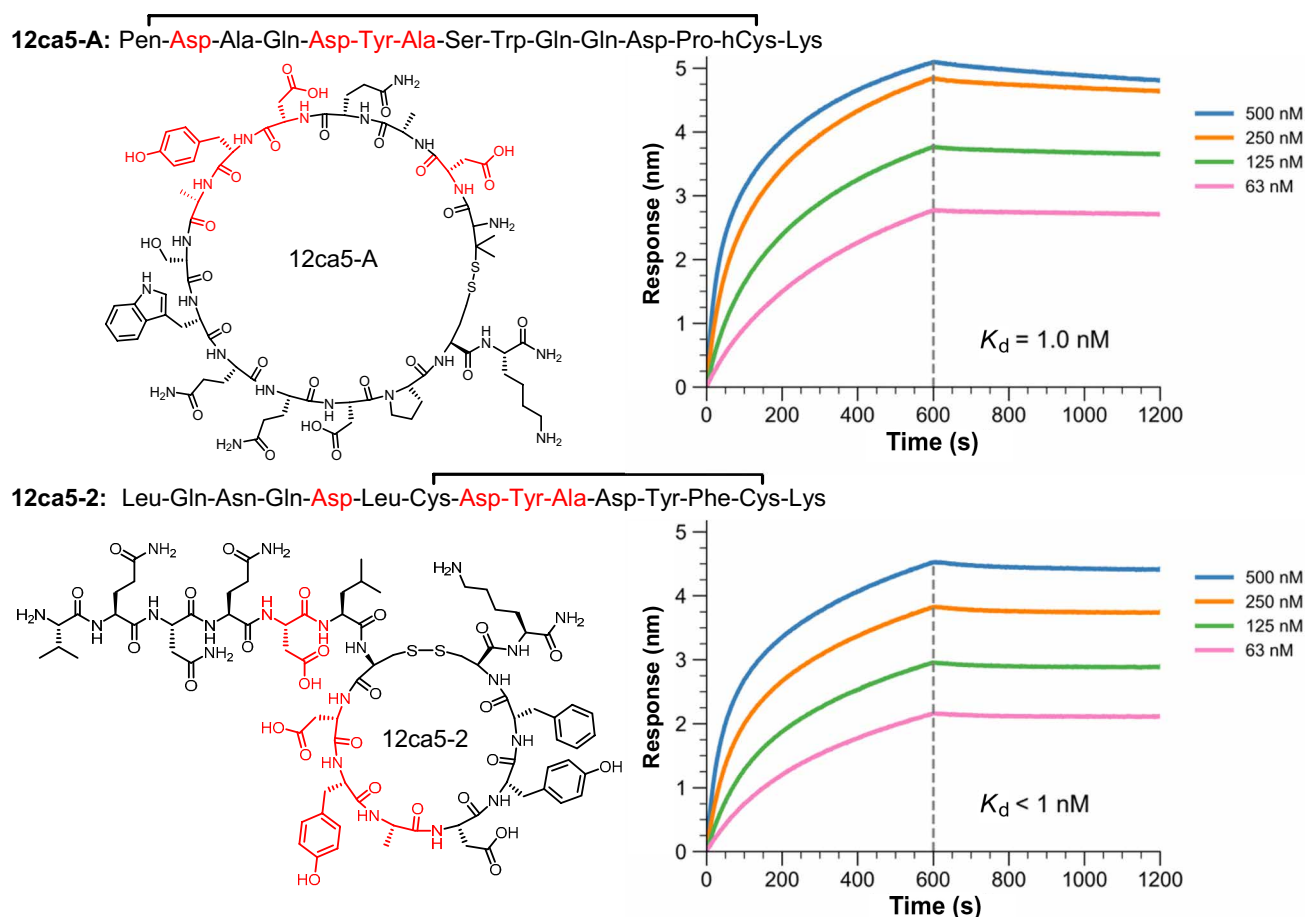


Fig. 4. High-affinity macrocyclic peptide ligands to 12ca5 are enriched and identified via AS-MS, and the binding affinity is confirmed and measured using BLI. All peptides were prepared with Lys(biotin)–aminohexanoic acid (Ahx) attached to the N terminus of the shown sequence and immobilized onto the BLI tip. The BLI tip was then dipped into solutions containing varying concentrations of 12ca5 to record the concentration-dependent association and dissociation events. The characteristic 12ca5-binding motif D**DY(A/S) is highlighted in red and appeared exclusively at a single position in the X_6CX_6CK library (seven discovered peptides). In comparison, only one motif-containing peptide was discovered from the $CX_{12}CK$ library.

protein. One peptide with high sequencing confidence was identified as being enriched against CDH2 (KMTFLFCNFTYKDZK, called cadherin-binding peptide, **CBP**, where Z is penicillamine disulfide bonded to C). Notably, previous ligand discovery efforts against CDH2 using linear $X_{12}K$ libraries were unable to identify any ligands. **CBP** was synthesized and tested for its binding affinity to CDH2 by BLI, yielding a 53 nM K_d value (Fig. 5). To verify sequence binding specificity, a scramble sequence that preserved the size of the macrocycle was synthesized and shown to have negligible binding response to CDH2 by BLI (fig. S6). The linearized form of **CBP** was also tested and demonstrated minimal binding response (0.2-nM versus 1.6-nM response for the macrocycle), with an affinity of $K_d = 150$ nM (figs. S7 and S8). The more rigid structure of the macrocyclic **CBP**, thus, appears to favor higher affinity.

SARs were delineated to characterize **CBP** using single-residue replacement studies (alanine and D-amino acid scans) and truncations. In all SAR studies, the Cys⁷-Pen¹⁴ disulfide bond was maintained to provide a consistent macrocycle structure to optimize from. First, an alanine scan was performed by synthesis of 13 variants featuring individual alanine mutations, which were assayed by BLI against CDH2 (table S3 and fig. S9). This alanine scan revealed multiple residues to be important for binding (hotspots) including Lys⁴, Phe⁶, Lys¹², and Lys¹⁵, due to the complete ablation of binding to CDH2 observed in BLI assays (fig. S10). Other residues including Met², Thr³, Leu⁵, Thr¹⁰, Tyr¹¹, and Asp¹³ had no effect on binding (coldspots), suggesting that they are not drivers of **CBP** binding to CDH2. Second, a truncation study focused at shortening **CBP** from the N terminus, producing five additional peptides for BLI testing (table S4 and fig. S11). BLI assays with these peptides confirmed

the impact of the N-terminal residues on binding affinity, especially Phe⁶ as well as Leu⁵, while Met² and Thr³ contributed minimally to CDH2 binding (fig. S12). Third, a D-amino acid scan of **CBP** was performed by iteratively replacing L-amino acids with D-amino acids to determine the impact of stereochemistry on the ligand interactions (93, 94). Notable hotspots identified from the D-amino acid scan were Phe⁶ and Tyr¹¹, further reinforcing the importance of the aromatic residues for binding (see table S5 and figs. S13 and S14). In summary, these initial SAR studies outline the hotspot residues that appear to drive the high-affinity binding of **CBP** to CDH2, including Lys⁴, Phe⁶, Lys¹², and Lys¹⁵, while Met², Thr³, Leu⁵, Thr¹⁰, and Asp¹³ are designated as coldspots with a minimal effect on binding.

SAR data informed the design of two focused libraries based on **CBP**: one to derivatize the high-affinity hotspot residues and the other to derivatize the coldspot residues nonessential for binding. A previous approach to design noncanonical libraries is to diversify the hotspots (95, 96). However, peptide development and optimization often also considers the coldspot residues that do not drive high-affinity binding to the target. These coldspot residues can be non-intuitively critical to improving binding affinity, solubility, or proteolytic stability (61, 62). Thus, we chose to compare the results from both maturation strategies. The set of noncanonical amino acids for incorporation in both the hotspot and coldspot focused libraries were selected on the basis of the consensus data provided by the docking, alanine scan, D-amino acid scan, and truncation studies (Fig. 6, A and B). These libraries were synthesized and subjected to validation by SEC as shown in fig. S15 to demonstrate the lack of apparent oligomerization after disulfide bond formation.

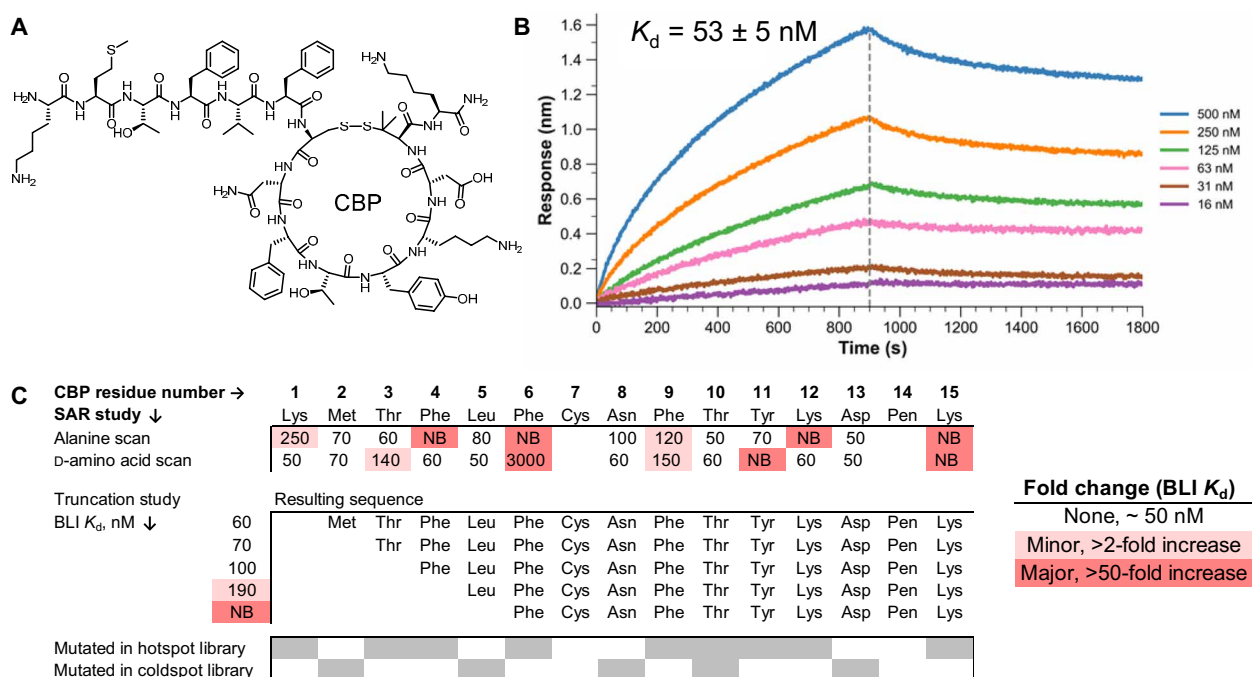


Fig. 5. Macrocyclic peptide libraries enable discovery of a 53 nM peptide ligand to a portion of the ectodomain of CDH2. (A) Structure of **CBP**. (B) BLI experiment reports the affinity of **CBP** to CDH2 with $K_d = 53$ nM binding affinity. All peptides were prepared with Lys(biotin)-Ahx attached to the N terminus in addition to the sequence shown and immobilized onto the BLI tip. The BLI tip was then dipped into solutions containing varying concentrations of CDH2 to record the concentration-dependent association and dissociation events. (C) Summary of experimental (alanine scan, D-amino acid scan, and N-terminal truncation study) SAR data. "NB" denotes nonbinding. This SAR information was used to inform the designation of **CBP** "hotspots" and "coldspots," which do or do not drive high-affinity binding, respectively.

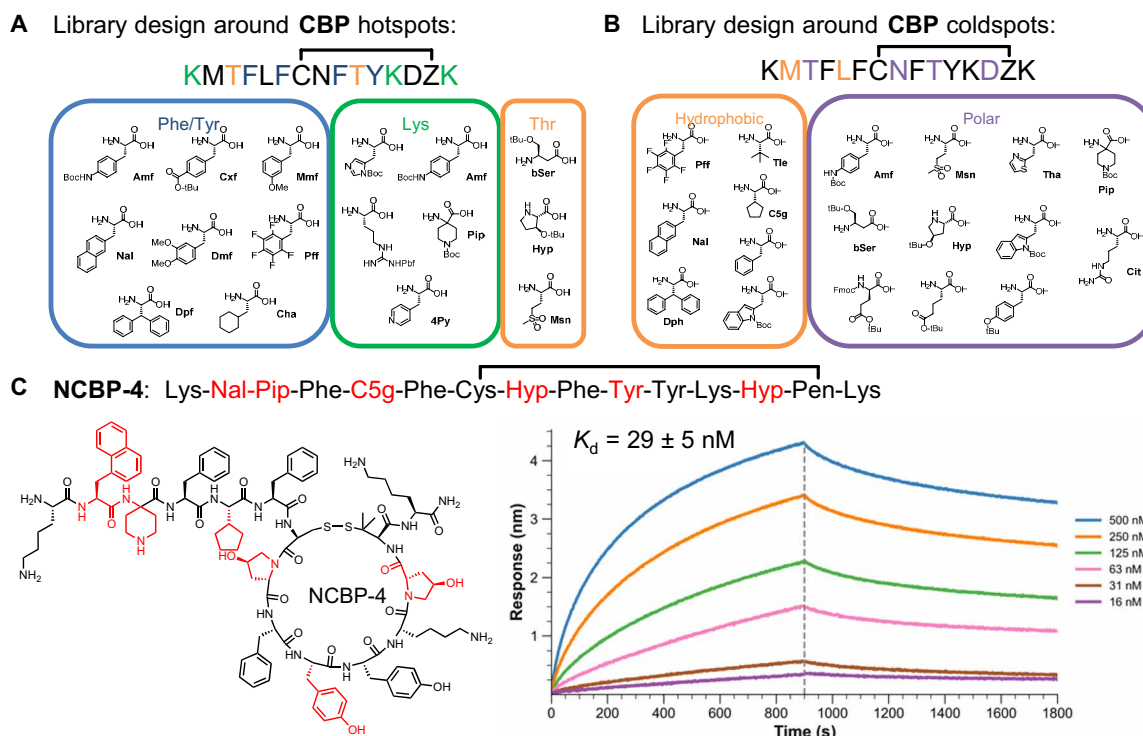


Fig. 6. Single-peptide SAR study informs combinatorial library design and affinity maturation with noncanonical amino acids. (A and B) From the single-peptide SAR studies summarized in Fig. 5C, two libraries were designed to perform affinity maturation. The first library focused on minimally derivatizing the hotspots by matching the original natural amino acids properties (e.g., hydrophobicity or positive charge). The second library focused around diversifying the coldspots to examine the possibility that these could be mutated to improve the overall binding of the **CBP** peptide. Both libraries were prepared using split-and-pool synthesis, except that the entirety of the theoretical sequence space was sampled by the library because of its lower diversity focused design. Specifically, the number of beads used in split-and-pool synthesis approximately matched the theoretical diversity: Hotspot library total number of beads: 2.5×10^6 with theoretical sequence space diversity: 2.7×10^6 and coldspot library total number of beads: 7.0×10^5 with theoretical sequence space diversity: 7.2×10^5 . (C) Sequence and structure of **NCBP-4** discovered from affinity selection and its BLI binding response, which exhibited high-affinity binding ($K_d = 29 \pm 5$ nM). Nal, 3-(2-naphthyl)-L-alanine; Pip, 4-aminopiperidine-4-carboxylic acid; C5g, cyclopentylglycine; Hyp, L-trans-4-hydroxyproline.

No high-affinity ligands were discovered from the hotspot focused library by AS-MS, while the coldspot library provided 10 high-affinity noncanonical macrocyclic CDH2 peptide binders (**NCBPs**). From the hotspot library, only two candidates were identified with high sequencing confidence, which featured multiple mutations from the original **CBP** sequence and shared replacements including Thr¹⁰ Msn, Tyr¹¹Dph, and Lys¹⁵Arg. However, the two hotspot candidates (**NCBP-1** and **NCBP-2**) were synthesized and tested by BLI, revealing that they were non-binders to CDH2 under these conditions (figs. S16 and S17). From the coldspot library, 10 noncanonical putative binders with high sequencing confidence were discovered and synthesized (table S6 and fig. S16). All discovered sequences from the coldspot library (**NCBP-3** to **NCBP-12**) were high-affinity binders to CDH2 in the BLI experiments, with determined K_d values between 20 and 50 nM (fig. S17). The improvement in binding affinities observed by BLI upon derivatization of the coldspot residues supports this strategy as an efficient avenue for further optimization.

The **NCBP-4** noncanonical binder exhibits nanomolar binding affinity to CDH2 ($K_d = 29 \pm 5$ nM). The results from AS-MS of the coldspot macrocyclic library show that most coldspot amino acids were replaced in the identified sequences (table S6). In all candidates, Met² was replaced by a hydrophobic amino acid, with 3-(2-naphthyl)-L-alanine (Nal) appearing in 6 of the 10. Similarly, Leu⁵ was replaced by Phe, Nal,

cyclopentylglycine (C5g), or pentafluoro-L-phenylalanine (PFf). For the polar subset of amino acids in the coldspot library, the replacements made to **CBP** were more mixed. Asn⁸ and Thr¹⁰ were replaced with a diverse set of amino acids, possibly indicating their lack of contribution to the binding interaction. Thr³ was replaced by cationic 4-aminopiperidine-4-carboxylic acid (Pip) and polar L-β-homoserine (bSer). Last, Asp¹³ demonstrated a preferred replacement to trans-4-hydroxyproline (Hyp), appearing in 5 of the 10 candidates. With these results in mind, **NCBP-4** was chosen for detailed investigation by BLI as it featured a consensus of amino acid replacements including Met²Nph, Thr³Pip, Leu⁵C5g, and Asp¹³Hyp (fig. S18). **NCBP-4** exhibited clear concentration-dependent binding to CDH2, and a resulting binding affinity of $K_d = 29 \pm 5$ nM was determined by BLI (Fig. 6). Moreover, **NCBP-4** demonstrated a stronger response illustrated by a higher BLI signal (~4.3 nm), more than double the response seen with **CBP** (~1.6 nm, fig. S19). Table S7 gives a summary of K_d measurements by BLI for **CBP** and derivatives.

As an additional control, a specific mutant of **NCBP-4** was constructed with serine mutated at the hotspots to specifically examine whether the coldspot residues were effective in creating unprecedented binding interactions with CDH2 (sequence: Ser-Nal-Pip-Ser-C5g-Ser-Cys-Hyp-Ser-Tyr-Ser-Ser-Hyp-Pen-Ser-NH₂). This mutant retained moderate binding to CDH2 with an apparent K_d of ~150 nM

(fig. S20). This serine-substituted mutant was also tested against 12ca5 to assess nonspecific binding. The mutant showed no affinity toward 12ca5 (fig. S19). This result suggests that the coldspot residues of CBP could have been optimized further in **NCBP-4** in AS-MS, as this control ligand demonstrates some binding to CDH2 without nonspecific binding.

In addition to increasing the affinity of **NCBP-4** to CDH2, the incorporation of unnatural amino acids also enhanced the peptide's proteolytic resistance to chymotrypsin. Cyclized samples of **CBP** and **NCBP-4** were incubated with chymotrypsin in a 50:1 ratio by mass for up to 30 min; subsequent liquid chromatography (LC)–MS analysis showed a 40-fold increase in half-life, with **CBP** showing a half-life of 5 min, while **NCBP-4** showed an estimated half-life of 200 min (see fig. S20). Analysis of the degradation products revealed the primary site of proteolysis for **CBP** to be at the Phe⁴-Leu⁵ junction in the linear portion of the peptide with a minor cleavage site at the Phe⁶-Cys⁷ junction, whereas potential cleavage sites within the cyclized portion, such as Phe⁹ or Tyr¹¹, demonstrated minimal cleavage (see figs. S20 to S22). Additionally, linearized full-length peptide was also observed. Proteolysis of **NCBP-4** by chymotrypsin yielded a major product corresponding to 18 Da greater than the cyclized mass, corresponding to hydrolysis. These studies exemplify the substantial increase in proteolytic stability imparted by the incorporation of unnatural amino acids.

DISCUSSION

We established a protocol for the split-and-pool synthesis of high-diversity macrocyclic peptide libraries and demonstrated their use in the discovery of nanomolar ligands against two protein targets of different structure. Formation of the macrocycle is performed using a simple disulfide bond, which is rapidly installed in aqueous solution using iodine. Quantification of free thiol content via Ellman's assay in both the cyclized and linearized forms confirmed the complete conversion of thiols to disulfides in the library, while SEC revealed that the disulfide bonds were formed exclusively intramolecularly without oligomerization. While the disulfide bond is not the most robust linkage for cyclization, there are several approaches available to replace it when needed to improve stability toward therapeutic development (11, 97, 98). Such a strategy would require control over bond distances. However, due to their increased chemical stability, linkages such as thioethers and lactamization can be challenging to linearize, needing harsh conditions or fixed amino acids (70–75). The disulfide linkage is shown to be compatible with the inclusion of unnatural thiol-containing residues while also not adding any additional steps to the library synthesis and preparation.

Affinity selection was able to identify protein-specific ligands from these synthetic macrocyclic libraries for both a model protein (12ca5) and a second target, CDH2, which participates in basic biological adhesion of cells in neural and cardiometabolic function. Both the canonical **CBP** and noncanonical **NCBP-4** peptides demonstrated concentration-dependent binding to CDH2, binding specificity, and high affinity with K_d values of 50 and 29 nM, respectively. After examining the SAR of **CBP**, several hotspot residues were revealed to be critical for binding to CDH2, featuring several hydrophobic and cationic residues.

From the SAR studies, two additional macrocyclic libraries containing a diverse set of noncanonical amino acids were synthesized focusing on the affinity-driving hotspots and the nonessential coldspots, respectively. The subsequent affinity selection experiments investigated

the hypotheses of whether the hotspots can be further refined or whether the coldspots can become meaningful contributors to the binding affinity upon maturation with focused library designs. Overall, AS-MS using the hotspot CDH2-focused library did not provide any binders or improvement to the original **CBP** peptide. However, AS-MS experiments using the coldspot library were able to provide several candidates individually validated to be high-affinity binders. Of these, **NCBP-4** was examined more closely for its high affinity ($K_d \sim 29$ nM), specificity, and specific side-chain contributions demonstrated by the amino acids that replaced the original **CBP** coldspot residues.

Using noncanonical amino acids in combinatorically prepared macrocyclic libraries, we demonstrated the affinity maturation of **CBP**. This process was successful through the replacement of coldspot residues with noncanonical monomers. Overall, because of the improvements that macrocyclization often offers over linear peptide scaffolds, we expect this work to be fundamental to the impactful deployment of macrocyclic synthetic libraries for the advancement of peptide therapeutics discovery and development.

MATERIALS AND METHODS

Rapid oxidation of peptide thiols for intramolecular cyclization using iodine

Additional information is included in the Supplementary Materials. Briefly, after cleavage and lyophilization, each split-and-pool prepared peptide library (e.g., 10 mg, 4.2 μ mol, and average molecular weight ~ 2400 g/mol) was resuspended at 2 mg/ml in 5% AcN in water [0.1% trifluoroacetic acid (TFA)] and treated with 10 μ l portions of freshly prepared 60 mM I₂ in MeOH until the solution remained yellow. For the example 10-mg scale, ~ 70 μ l I₂ stock solution total was used, resulting in ~ 1 equiv. of I₂ with respect to the library. The iodine-treated library was incubated for 10 min in the dark at room temperature, upon which 15 μ l of freshly prepared 1 M ascorbic acid was added (~ 3.6 equiv. of ascorbic acid with respect to the library example). This solution was immediately loaded onto a pre-equilibrated SPE column, SPE purified to remove any remaining iodine and ascorbic acid, and lyophilized. The lyophilized powder was then resuspended at ~ 0.1 mM and its thiol concentration was quantified by Ellman's assay.

Reductive linearization of cyclized library

Peptide libraries were resuspended at 0.62 mg/ml to mimic the maximum concentration possibly isolated at the end of AS-MS, due to the maximum capacity of the StageTip (8 μ g for a double plug, using 13 μ l). As described in the Results, reduction after resuspension at pH 3 from 0.1% formic acid in ultrapure water was successful using 1,4-DL-DTT (Chem-Impex, catalog no. 00127). The reduction was also tested in 200 mM sodium phosphate, 5 mM EDTA, pH 8 with DTT, and immobilized TCEP (Thermo Fisher Scientific, 77712). DTT was freshly prepared as a stock solution of 500 mg/ml, added to samples to provide a solution of 50 mg/ml final concentration (1000 equiv.), and incubated at 60°C for 15 min. Samples were then SPE purified, lyophilized, and Ellman's assay quantified upon resuspension. Immobilized TCEP beads (8 mM stock suspension) were washed three times before use with the assay buffer using centrifugation at $1000 \times g$ (relative centrifugal force, rcf) for 1 min. Treatment of the library peptides with immobilized TCEP used 20 equiv. for 25 min at room temperature rocking on a nutating mixer. The supernatant was isolated from centrifugation, lyophilized, and

Ellman's quantified. Additional information is included in the Supplementary Materials.

Sequencing validation of reduced and oxidized libraries

A small portion of library resin was measured and made into a stock solution of 1 mg/ml in *N,N'*-dimethylformamide (DMF). Several aliquots of ~1000 beads (for 20 μ m resin, this will be about ~10 μ l of 1 mg/ml stock) were taken, centrifuged, and aspirated of DMF. Each aliquot was cleaved from the solid-phase support using 60 μ l of 95% trifluoroacetic acid, 2.5% water, and 2.5% triisopropylsilane at 60°C for 15 min. Half of the liquid was then evaporated under a gentle stream of N_2 , followed by dilution to a total volume of 240 μ l using water (0.1% TFA). A third of the solution was aliquoted to represent the library before cyclization. The remaining solution was cyclized according to section 2.5 of the Supplementary Materials. The cyclized peptide library and aliquoted linear library were both prepared for nLC/MS-MS analysis according to section 2.4 of the Supplementary Materials. The dried library samples were then reconstituted in water (0.1% TFA) at a concentration of 100 pg/ μ l per peptide (for example, prepare 8 μ g of an aliquot of 1000 peptides in 80 μ l). Half of the cyclized peptide sample was then linearized using DTT as described in section 2.6 of the Supplementary Materials. All three types of samples—peptide post-cleavage, cyclized, and cyclized then reduced—were subjected to nano-flow LC-MS/MS analysis as described in the Supplementary Materials.

Ellman's thiol quantification assay

The thiol concentration of suspended peptides was determined using Ellman's reagent [MilliporeSigma, 5,5'-dithiobis(2-nitrobenzoic acid), D8130, $\geq 98\%$, BioReagent] using the following conditions. Ellman's stock solution was prepared at 10.0 mM, and assay buffer was 1 \times phosphate-buffered saline (PBS) at pH 8.0 with 1 mM of EDTA. Nonsterile Greiner 96-well polystyrene plates (MilliporeSigma, M2936) were used. Using the assay buffer to have a final 200- μ l well volume, 3.6 μ l of Ellman's stock solution was combined with the peptide solution to give a final peptide intended concentration of 0.1 mM, which was determined to be within the linear regime in which signal could be observed from a standard curve constructed using cysteine (MilliporeSigma, C7352, $\geq 98\%$, BioReagent). After combining, all materials were incubated for 7 min and analyzed by recording absorbance at 416 nm using a TECAN Spark Plate Reader. The concentration of the library was inferred by measuring its absorbance at 280 nm (NanoQuant Plate) and was used to normalize the Ellman's thiol concentration to account for slight variations in the intended resuspended concentrations. Sample preparation to measure thiol signal from cleavage and SPE of library (reduced library): Approximately 50 mg of peptide library (peptide + resin) was globally deprotected and cleaved from resin with 95% (v/v) TFA, 2.5% (v/v) water, and 2.5% (v/v) triisopropylsilane, for 15 min at 60°C (~20 ml/g of resin). Precipitated peptide was triturated (3 \times 100 ml/g of resin) with cold diethyl ether, resuspended in 5% acetonitrile in water (0.1% TFA), and solid-phase extracted. After lyophilization, this sample was resuspended in assay buffer at 0.1 mM and measured for its thiol concentration by Ellman's assay.

SEC of libraries

SEC was performed using an Agilent 1260 Infinity II LC System with a Superdex 30 Increase 10/300 GL column (10 mm by 300 mm, 9- μ m particle size from Cytiva Life Sciences, separation M_w range of

100 to 7000 Da). Library (25 μ g) was injected in 200 μ l of total solution. Cyclized peptide samples were aliquoted from the main stock prepared according to sections 2.3 and 2.5 of the Supplementary Materials. Linearized samples were prepared by adding 1000 equiv. from a DTT stock solution of 50 mg/ml and heating the sample to 60°C for 10 min before dilution to 200 μ l using 1 \times PBS. Column conditions: isocratic 1 \times PBS for 1.5 column volumes at 0.8 ml/min. Buffer blanks were prepared for both cyclized and linearized samples and were subtracted from the library samples. A custom mass standard was prepared by adding 10 μ g of a mixture of peptides corresponding to the following molecular weights: 1807, 3750, and 5312 Da for average monomer mass, average dimer mass, and average trimer mass. The sequences are as follows:

1. SQETFSDLWKLLPEN: molecular weight of 1807 Da
2. HGPATPRMAKFDQAAGDQYMAGMDKRKAGRAAGATL: molecular weight of 3750 Da
3. MNSTESIPLAQSTVAQSTVAGFTSELESTPVPSNETTCEN-WREIHHLVFHVA: molecular weight of 5685 Da

Supplementary Materials

This PDF file includes:

Supplementary Materials and Methods

Figs. S1 to S22

Tables S1 to S7

References

REFERENCES AND NOTES

1. A. D. Cunningham, N. Qvit, D. Mochly-Rosen, Peptides and peptidomimetics as regulators of protein-protein interactions. *Curr. Opin. Struct. Biol.* **44**, 59–66 (2017).
2. J. A. Wells, C. L. McClendon, Reaching for high-hanging fruit in drug discovery at protein-protein interfaces. *Nature* **450**, 1001–1009 (2007).
3. A. Henninot, J. C. Collins, J. M. Nuss, The current state of peptide drug discovery: Back to the future? *J. Med. Chem.* **61**, 1382–1414 (2018).
4. M. Muttenthaler, G. F. King, D. J. Adams, P. F. Alewood, Trends in peptide drug discovery. *Nat. Rev. Drug Discov.* **20**, 309–325 (2021).
5. M. Góngora-Benítez, J. Tulla-Puche, F. Albericio, Multifaceted roles of disulfide bonds. Peptides as therapeutics. *Chem. Rev.* **114**, 901–926 (2014).
6. A. A. Vinogradov, Y. Yin, H. Suga, Macrocyclic peptides as drug candidates: Recent progress and remaining challenges. *J. Am. Chem. Soc.* **141**, 4167–4181 (2019).
7. J. D. A. Tyndall, T. Nall, D. P. Fairlie, Proteases universally recognize beta strands in their active sites. *Chem. Rev.* **105**, 973–999 (2005).
8. D. P. Fairlie, J. D. A. Tyndall, R. C. Reid, A. K. Wong, G. Abbenante, M. J. Scanlon, D. R. March, D. A. Bergman, C. L. L. Chai, B. A. Burkett, Conformational selection of inhibitors and substrates by proteolytic enzymes: Implications for drug design and polypeptide processing. *J. Med. Chem.* **43**, 1271–1281 (2000).
9. D. Wang, W. Liao, P. S. Arora, Enhanced metabolic stability and protein-binding properties of artificial α helices derived from a hydrogen-bond surrogate: Application to Bcl-xL. *Angew. Chem. Int. Ed. Engl.* **44**, 6525–6529 (2005).
10. A. M. Spokoyin, Y. Zou, J. J. Ling, H. Yu, Y. S. Lin, B. L. Pentelute, A perfluoroaryl-cysteine SNAr chemistry approach to unprotected peptide stapling. *J. Am. Chem. Soc.* **135**, 5946–5949 (2013).
11. R. Tugyi, G. Mezö, E. Fellingner, D. Andreu, F. Hudecz, The effect of cyclization on the enzymatic degradation of herpes simplex virus glycoprotein D derived epitope peptide. *J. Pept. Sci.* **11**, 642–649 (2005).
12. L. D. Walensky, A. L. Kung, I. Escher, T. J. Malia, S. Barbuto, R. D. Wright, G. Wagner, G. L. Verdine, S. J. Korsmeyer, Activation of apoptosis in vivo by a hydrocarbon-stapled BH3 helix. *Science* **305**, 1466–1470 (2004).
13. M. R. Naylor, A. T. Bockus, M. J. Blanco, R. S. Lokey, Cyclic peptide natural products chart the frontier of oral bioavailability in the pursuit of undruggable targets. *Curr. Opin. Chem. Biol.* **38**, 141–147 (2017).
14. C. R. Pye, W. M. Hewitt, J. Schwochert, T. D. Haddad, C. E. Townsend, L. Etienne, Y. Lao, C. Limberakis, A. Furukawa, A. M. Mathiowetz, D. A. Price, S. Liras, R. S. Lokey, Nonclassical size dependence of permeation defines bounds for passive adsorption of large drug molecules. *J. Med. Chem.* **60**, 1665–1672 (2017).
15. G. Bhardwaj, J. O'Connor, S. Rettie, Y. H. Huang, T. A. Ramelot, V. K. Mulligan, G. G. Alpkilic, J. Palmer, A. K. Bera, M. J. Bick, M. Di Piazza, X. Li, P. Hosseinzadeh, T. W. Craven, R. Tejoro,

- A. Lauko, R. Choi, C. Glynn, L. Dong, R. Griffin, W. C. van Voorhis, J. Rodríguez, L. Stewart, G. T. Montelione, D. Craik, D. Baker, Accurate de novo design of membrane-traversing macrocycles. *Cell* **185**, 3520–3532.e26 (2022).
16. M. Mizuno-Kaneko, I. Hashimoto, K. Miyahara, M. Kochi, N. Ohashi, K. Tsumura, K. Suzuki, T. Tamura, Molecular design of cyclic peptides with cell membrane permeability and development of MDMX-p53 inhibitor. *ACS Med. Chem. Lett.* **14**, 1174–1178 (2023).
17. S. E. Iskandar, A. A. Bowers, mRNA display reaches for the clinic with new PCSK9 inhibitor. *ACS Med. Chem. Lett.* **13**, 1379–1383 (2022).
18. G. Bourne, A. Bhandari, X. Cheng, B. Frederick, J. Zhang, D. Patel, D. Liu, Oral peptide inhibitors of interleukin-23 receptor and their use to treat inflammatory bowel diseases. Patent US9624268B2 (2017).
19. R. I. Benhamou, S. Vezina-Dawod, S. Choudhary, K. W. Wang, S. M. Meyer, I. Yildirim, M. D. Disney, Macrocyclization of a ligand targeting a toxic RNA dramatically improves potency. *ChemBioChem* **21**, 3229–3233 (2020).
20. D. E. Hacker, N. A. Abrigo, J. Hoinka, S. L. Richardson, T. M. Przytycka, M. C. T. Hartman, Direct, competitive comparison of linear, monocyclic, and bicyclic libraries using mRNA display. *ACS Comb. Sci.* **22**, 306–310 (2020).
21. Y. Gao, T. Kodadek, Direct comparison of linear and macrocyclic compound libraries as a source of protein ligands. *ACS Comb. Sci.* **17**, 190–195 (2015).
22. T. Passioura, T. Katoh, Y. Goto, H. Suga, Selection-based discovery of druglike macrocyclic peptides. *Annu. Rev. Biochem.* **83**, 727–752 (2014).
23. A. Tavassoli, SICLOPPS cyclic peptide libraries in drug discovery. *Curr. Opin. Chem. Biol.* **38**, 30–35 (2017).
24. Y. Goto, H. Suga, The RaPID platform for the discovery of pseudo-natural macrocyclic peptides. *Acc. Chem. Res.* **54**, 3604–3617 (2021).
25. K. Deyle, X. D. Kong, C. Heinis, Phage selection of cyclic peptides for application in research and drug development. *Acc. Chem. Res.* **50**, 1866–1874 (2017).
26. K. Bacon, A. Blain, M. Burroughs, N. McArthur, B. M. Rao, S. Menegatti, Isolation of chemically cyclized peptide binders using yeast surface display. *ACS Comb. Sci.* **22**, 519–532 (2020).
27. J. Y. K. Wong, R. Mukherjee, J. Miao, O. Bilyk, V. Triana, M. Miskolzie, A. Henninot, J. J. Dwyer, S. Kharchenko, A. Iampolska, D. M. Volochnyuk, Y. S. Lin, L. M. Postovit, R. Derda, Genetically-encoded discovery of proteolytically stable bicyclic inhibitors for morphogen NODAL. *Chem. Sci.* **12**, 9694–9703 (2021).
28. A. E. Owens, J. A. Iannuzzelli, Y. Gu, R. Fasan, MORPH-PhD: An integrated phage display platform for the discovery of functional genetically encoded peptide macrocycles. *ACS Cent. Sci.* **6**, 368–381 (2020).
29. É. Biron, S. Vézina-Dawod, F. Bédard, “Synthetic strategies for macrocyclic peptides” in *Practical Medicinal Chemistry with Macrocycles*, E. Marsault, M. L. Peterson, Eds. (Wiley, 2017), pp. 205–241.
30. S. Habeshian, M. L. Merz, G. Sangouard, G. K. Mothukuri, M. Schüttel, Z. Bognár, C. Diaz-Perlas, J. Vesin, J. Bortoli Chapalay, G. Turcatti, L. Cendron, A. Angelini, C. Heinis, Synthesis and direct assay of large macrocycle diversities by combinatorial late-stage modification at picomole scale. *Nat. Commun.* **13**, 3823 (2022).
31. S. Pomplun, M. Jbara, A. J. Quartararo, G. Zhang, J. S. Brown, Y. C. Lee, X. Ye, S. Hanna, B. L. Pentelute, De novo discovery of high-affinity peptide binders for the SARS-CoV-2 spike protein. *ACS Cent. Sci.* **7**, 156–163 (2021).
32. G. Zhang, J. S. Brown, A. J. Quartararo, C. Li, X. Tan, S. Hanna, S. Antilla, A. E. Cowfer, A. Loas, B. L. Pentelute, Rapid de novo discovery of peptidomimetic affinity reagents for human angiotensin converting enzyme 2. *Commun. Chem.* **5**, 8 (2022).
33. A. J. Quartararo, Z. P. Gates, B. A. Somsen, N. Hartrampf, X. Ye, A. Shimada, Y. Y. Kajihara, C. Ottmann, B. L. Pentelute, Ultra-large chemical libraries for the discovery of high-affinity peptide binders. *Nat. Commun.* **11**, 3183 (2020).
34. C. J. White, A. K. Yudin, Contemporary strategies for peptide macrocyclization. *Nat. Chem.* **3**, 509–524 (2011).
35. A. I. Ekanayake, L. Sobze, P. Kelich, J. Youk, N. J. Bennett, R. Mukherjee, A. Bhardwaj, F. Wuest, L. Vukovic, R. Derda, Genetically encoded fragment-based discovery from phage-displayed macrocyclic libraries with genetically encoded unnatural pharmacophores. *J. Am. Chem. Soc.* **143**, 5497–5507 (2021).
36. N. C. Wrighton, F. X. Farrell, R. Chang, A. K. Kashyap, F. P. Barbone, L. S. Mulcahy, D. L. Johnson, R. W. Barrett, L. K. Jolliffe, W. J. Dower, Small peptides as potent mimetics of the protein hormone erythropoietin. *Science* **273**, 458–463 (1996).
37. W. J. Fairbrother, H. W. Christinger, A. G. Cochran, G. Fuh, C. J. Keenan, C. Quan, S. K. Shriver, J. Y. K. Tom, J. A. Wells, B. C. Cunningham, Novel peptides selected to bind vascular endothelial growth factor target the receptor-binding site. *Biochemistry* **37**, 17754–17764 (1998).
38. W. L. DeLano, M. H. Ultsch, A. M. De Vos, J. A. Wells, Convergent solutions to binding at a protein-protein interface. *Science* **287**, 1279–1283 (2000).
39. H. Zhang, S. Chen, Cyclic peptide drugs approved in the last two decades (2001–2021). *RSC Chem. Biol.* **3**, 18–31 (2022).
40. O. Ovadia, S. Greenberg, B. Laufer, C. Gilon, A. Hoffman, H. Kessler, Improvement of drug-like properties of peptides: The somatostatin paradigm. *Expert Opin. Drug Discovery* **5**, 655–671 (2010).
41. M. Glavaš, A. Gitlin-Domagalska, D. Dębowski, N. Ptaszyńska, A. Łęgowska, K. Rolka, Vasopressin and its analogues: From natural hormones to multitasking peptides. *Int. J. Mol. Sci.* **23**, 3068 (2022).
42. D. H. Copp, Calcitonin: Discovery, development, and clinical application. *Clin. Invest. Med.* **17**, 268–277 (1994).
43. K. Sakamoto, T. Masutani, T. Hirokawa, Generation of KS-58 as the first K-Ras(G12D)-inhibitory peptide presenting anti-cancer activity in vivo. *Sci. Rep.* **10**, 21671 (2020).
44. P. J. Kner, A. Tzekou, D. Ricklin, H. Qu, H. Chen, W. A. van der Donk, J. D. Lambris, Synthesis and activity of Thioether-containing analogues of the complement inhibitor compstatin. *ACS Chem. Biol.* **6**, 753–760 (2011).
45. J. P. Fischer, R. Schönauer, S. Els-Heindl, D. Bierter, J. Koebberling, B. Riedl, A. G. Beck-Sickinger, Adrenomedullin disulfide bond mimetics uncover structural requirements for AM₁ receptor activation. *J. Pept. Sci.* **25**, e3147 (2019).
46. J. Bondebjerg, M. Grunnet, T. Jespersen, M. Meldal, Solid-phase synthesis and biological activity of a Thioether analogue of conotoxin G1. *ChemBioChem* **4**, 186–194 (2003).
47. Z. V. F. Wright, S. McCarthy, R. Dickman, F. E. Reyes, S. Sanchez-Martinez, A. Cryar, I. Kilford, A. Hall, A. K. Takle, M. Topf, T. Gonen, K. Thalassinos, A. B. Tabor, The role of disulfide bond replacements in analogues of the tarantula toxin ProTx-II and their effects on inhibition of the voltage-gated sodium ion channel Nav1.7. *J. Am. Chem. Soc.* **139**, 13063–13075 (2017).
48. B. Hargittai, N. A. Solé, D. R. Groebe, S. N. Abramson, G. Barany, Chemical syntheses and biological activities of lactam analogues of α -conotoxin SI. *J. Med. Chem.* **43**, 4787–4792 (2000).
49. K. Aoki, M. Maeda, T. Nakae, Y. Okada, K. Ohya, K. Chiba, A disulfide bond replacement strategy enables the efficient design of artificial therapeutic peptides. *Tetrahedron* **70**, 7774–7779 (2014).
50. Y. K. Qi, Q. Qu, D. Bierter, L. Liu, A diaminodiacid (DADA) strategy for the development of disulfide surrogate peptides. *Chem. Asian J.* **15**, 2793–2802 (2020).
51. A. J. Robinson, B. J. van Lierop, R. D. Garland, E. Teoh, J. Elaridi, J. P. Illesinghe, W. R. Jackson, Regioselective formation of interlocked dicarba bridges in naturally occurring cyclic peptide toxins using olefin metathesis. *Chem. Commun.* **45**, 4293–4295 (2009).
52. J. L. Stymiest, B. F. Mitchell, S. Wong, J. C. Vederas, Synthesis of biologically active dicarba analogues of the peptide hormone oxytocin using ring-closing metathesis. *Org. Lett.* **5**, 47–49 (2003).
53. K. K. A. Reddy, D. K. Sahoo, S. Moi, K. H. Gowd, Conformational change due to replacement of disulfide with selenosulfide and diselenide in dipeptide vicinal cysteine loop. *Comput. Biol. Chem.* **97**, 107635 (2022).
54. L. Moroder, Isosteric replacement of sulfur with other chalcogens in peptides and proteins. *J. Pept. Sci.* **11**, 187–214 (2005).
55. A. Gori, P. Gagni, S. Rinaldi, Disulfide bond mimetics: Strategies and challenges. *Chem. Eur. J.* **23**, 14987–14995 (2017).
56. K. Holland-Nell, M. Meldal, Maintaining biological activity by using triazoles as disulfide bond mimetics. *Angew. Chem. Int. Ed. Engl.* **50**, 5204–5206 (2011).
57. S. Tomassi, A. M. Trotta, C. Ierano, F. Merlino, A. Messere, G. Rea, F. Santoro, D. Brancaccio, A. Carotenuto, V. M. D’Amore, F. S. Di Leva, E. Novellino, S. Cosconati, L. Marinelli, S. Scala, S. D. Maro, Disulfide bond replacement with 1,4- and 1,5-disubstituted [1,2,3]-triazole on C-X-C chemokine receptor type 4 (CXCR4) peptide ligands: Small changes that make big differences. *Chem. A Eur. J.* **26**, 10113–10125 (2020).
58. C. A. MacRaid, J. Illesinghe, B. J. Van Lierop, A. L. Townsend, M. Chebib, B. G. Livett, A. J. Robinson, R. S. Norton, Structure and activity of (2,8)-dicarba-(3,12)-cystino α -Iml, an α -conotoxin containing a nonreducible cystine analogue. *J. Med. Chem.* **52**, 755–762 (2009).
59. K. T. Mortensen, T. J. Osberger, T. A. King, H. F. Sore, D. R. Spring, Strategies for the diversity-oriented synthesis of macrocycles. *Chem. Rev.* **119**, 10288–10317 (2019).
60. C. Sayago, I. C. Gonzalez Valcarcel, Y. Qian, J. Lee, J. Alsina-Fernandez, N. C. Fite, J. J. Carrillo, F. F. Zhang, M. J. Chalmers, J. A. Dodge, H. Broughton, A. Espada, Deciphering binding interactions of IL-23R with HDX-MS: Mapping protein and macrocyclic dodecapeptide ligands. *ACS Med. Chem. Lett.* **9**, 912–916 (2018).
61. V. Guerlavais, T. K. Sawyer, L. Carvajal, Y. S. Chang, B. Graves, J.-G. Ren, D. Sutton, K. A. Olson, K. Packman, K. Darlak, C. Elkin, E. Feyfant, K. Kesavan, P. Gangurde, L. T. Vassilev, H. M. Nash, V. Vukovic, M. Aivado, D. A. Annis, Discovery of sulanemadlin (ALRN-6924), the first cell-permeating, stabilized α -helical peptide in clinical development. *J. Med. Chem.* **66**, 9401–9417 (2023).
62. M. Garrigou, B. Sauvagnat, R. Duggal, N. Boo, P. Gopal, J. M. Johnston, A. Partridge, T. Sawyer, K. Biswas, N. Boyer, Accelerated identification of cell active KRAS inhibitory macrocyclic peptides using mixture libraries and Automated Ligand Identification System (ALIS) technology. *J. Med. Chem.* **65**, 8961–8974 (2022).
63. S. Lim, N. Boyer, N. Boo, C. Huang, G. Venkatachalam, Y. C. A. Juang, M. Garrigou, H. Y. K. Kaan, R. Duggal, K. M. Peh, A. Sadruddin, P. Gopal, T. Y. Yuen, S. Ng, S. Kannan, C. J. Brown, C. S. Verma, P. Orth, A. Peier, L. Ge, X. Yu, B. Bhatt, F. Chen, E. Wang, N. J. Li, R. J. Gonzales, A. Stoeck, B. Henry, T. K. Sawyer, D. P. Lane, C. W. Johannes, K. Biswas,

- A. W. Partridge, Discovery of cell active macrocyclic peptides with on-target inhibition of KRAS signaling. *Chem. Sci.* **12**, 15975–15987 (2021).
64. A. Bruce, V. Adebomi, P. Czabala, J. Palmer, W. M. McFadden, Z. C. Lorson, R. L. Slack, G. Bhardwaj, S. G. Sarafianos, M. Raj, A tag-free platform for synthesis and screening of cyclic peptide libraries. *Angew. Chem. Int. Ed. Engl.* **63**, e202320045 (2024).
 65. R. J. Fair, R. T. Walsh, C. D. Hupp, The expanding reaction toolkit for DNA-encoded libraries. *Bioorg. Med. Chem. Lett.* **51**, 128339 (2021).
 66. B. Behsaz, H. Mohimani, A. Gurevich, A. Pribelski, M. Fisher, F. Vargas, L. Smarr, P. C. Dorrestein, J. S. Mylne, P. A. Pevzner, De novo peptide sequencing reveals many cyclopeptides in the human gut and other environments. *Cell Syst.* **10**, 99–108.e5 (2020).
 67. C. Townsend, A. Furukawa, J. Schwachert, C. R. Pye, Q. Edmondson, R. S. Lokey, CycLS: Accurate, whole-library sequencing of cyclic peptides using tandem mass spectrometry. *Bioorg. Med. Chem.* **26**, 1232–1238 (2018).
 68. D. Kavan, M. Kuzma, K. Lemr, K. A. Schug, V. Havlicek, CYCLONE - A utility for de novo sequencing of microbial cyclic peptides. *J. Am. Soc. Mass Spectrom.* **24**, 1177–1184 (2013).
 69. H. Mohimani, W. T. Liu, J. S. Mylne, A. G. Poth, M. L. Colgrave, D. Tran, M. E. Selsted, P. C. Dorrestein, P. A. Pevzner, Cycloquest: Identification of cyclopeptides via database search of their mass spectra against genome databases. *J. Proteome Res.* **10**, 4505–4512 (2011).
 70. J. H. Lee, A. M. Meyer, H. S. Lim, A simple strategy for the construction of combinatorial cyclic peptide libraries. *Chem. Commun.* **46**, 8615–8617 (2010).
 71. X. Liang, S. Vézina-Dawod, F. Bédard, K. Porte, E. Biron, One-pot photochemical ring-opening/cleavage approach for the synthesis and decoding of cyclic peptide libraries. *Org. Lett.* **18**, 1174–1177 (2016).
 72. A. Borges, C. Nguyen, M. Letendre, I. Onasenko, R. Kandler, N. K. Nguyen, J. Chen, T. Allakhverdova, E. Atkinson, B. DiChiara, C. Wang, N. Petler, H. Patel, D. Nanavati, S. Das, A. Nag, Facile de novo sequencing of tetrazine-cyclized peptides through UV-induced ring-opening and cleavage from the solid phase. *ChemBioChem* **24**, e202200590 (2023).
 73. L. S. Simpson, T. Kodadek, A cleavable scaffold strategy for the synthesis of one-bead one-compound cyclic peptide libraries that can be sequenced by tandem mass spectrometry. *Tetrahedron Lett.* **53**, 2341–2344 (2012).
 74. H. E. Elashal, R. D. Cohen, H. E. Elashal, M. Raj, Oxazolidinone-mediated sequence determination of one-bead one-compound cyclic peptide libraries. *Org. Lett.* **20**, 2374–2377 (2018).
 75. S. Menegatti, K. L. Ward, A. D. Naik, W. S. Kish, R. K. Blackburn, R. G. Carbonell, Reversible cyclic peptide libraries for the discovery of affinity ligands. *Anal. Chem.* **85**, 9229–9237 (2013).
 76. J. Novák, K. Lemr, K. A. Schug, V. Havlíček, CycloBranch: De novo sequencing of nonribosomal peptides from accurate product ion mass spectra. *J. Am. Soc. Mass Spectrom.* **26**, 1780–1786 (2015).
 77. N. H. Tran, R. Qiao, L. Xin, X. Chen, C. Liu, X. Zhang, B. Shan, A. Ghodsi, M. Li, Deep learning enables de novo peptide sequencing from data-independent-acquisition mass spectrometry. *Nat. Methods* **16**, 63–66 (2018).
 78. Y. Yamagishi, I. Shoji, S. Miyagawa, T. Kawakami, T. Katoh, Y. Goto, H. Suga, Natural product-like macrocyclic N-methyl-peptide inhibitors against a ubiquitin ligase uncovered from a ribosome-expressed de novo library. *Chem. Biol.* **18**, 1562–1570 (2011).
 79. J. M. Rini, U. Schulze-Gahmen, I. A. Wilson, Structural evidence for induced fit as a mechanism for antibody-antigen recognition. *Science* **255**, 959–965 (1992).
 80. R. A. Houghten, C. Pinilla, S. E. Blondelle, J. R. Appel, C. T. Dooley, J. H. Cuervo, Generation and use of synthetic peptide combinatorial libraries for basic research and drug discovery. *Nature* **354**, 84–86 (1991).
 81. J. S. Brown, S. Mohapatra, M. A. Lee, R. Misteli, Y. Tseo, N. M. Grob, A. J. Quartararo, A. Loas, R. Gomez-Bombarelli, B. L. Pentelute, Unsupervised machine learning leads to an abiotic picomolar peptide ligand. *ChemRxiv [Preprint]* (2023). <https://doi.org/10.26434/chemrxiv-2023-tws4n>.
 82. M. Takeichi, The cadherin superfamily in neuronal connections and interactions. *Nat. Rev. Neurosci.* **8**, 11–20 (2006).
 83. I. Kostetskii, J. Li, Y. Xiong, R. Zhou, V. A. Ferrari, V. V. Patel, J. D. Molkentin, G. L. Radice, Induced deletion of the N-cadherin gene in the heart leads to dissolution of the intercalated disc structure. *Circ. Res.* **96**, 346–354 (2005).
 84. M. Karlsson, C. Zhang, L. Méar, W. Zhong, A. Digre, B. Katona, E. Sjöstedt, L. Butler, J. Odeberg, P. Dusart, P. Edfors, P. Oksvold, K. von Feilitzen, M. Zwahlen, M. Arif, O. Altay, X. Li, M. Ozcan, A. Mardinoglu, L. Fagerberg, J. Mulder, Y. Luo, F. Ponten, M. Uhlen, C. Lindskog, A single-cell type transcriptomics map of human tissues. *Sci. Adv.* **7**, eabh2169 (2021).
 85. E. J. Williams, G. Williams, B. Gour, O. Blaschuk, P. Doherty, INP, a novel N-cadherin antagonist targeted to the amino acids that flank the HAV motif. *Mol. Cell. Neurosci.* **15**, 456–464 (2000).
 86. S. M. Burden-Gulley, T. J. Gates, S. E. L. Craig, S. F. Lou, S. A. Oblander, S. Howell, M. Gupta, S. M. Brady-Kalnay, Novel peptide mimetic small molecules of the HAV motif in N-cadherin inhibit N-cadherin-mediated neurite outgrowth and cell adhesion. *Peptides* **30**, 2380–2387 (2009).
 87. J. P. Tam, C. R. Wu, W. Liu, J. W. Zhang, Disulfide bond formation in peptides by dimethyl sulfoxide. scope and applications. *J. Am. Chem. Soc.* **113**, 6657–6662 (1991).
 88. M. C. Hennion, Solid-phase extraction: Method development, sorbents, and coupling with liquid chromatography. *J. Chromatogr. A* **856**, 3–54 (1999).
 89. Y. Yang, L. Hansen, A. Fraczek, F. Badalassi, J. Kjellström, DMF-assisted iodination side reaction during the preparation of disulfide peptides, its substrate/solvent/pH dependence, and implications on disulfide-peptide production. *Org. Process Res. Dev.* **25**, 2090–2099 (2021).
 90. Thermo Scientific (Pierce Biotechnology), “Instructions: Immobilized TCEP disulfide reducing gel (cat 77712), version 1325.3 MAN0011439” (2023).
 91. J. Rappsilber, M. Mann, Y. Ishihama, Protocol for micro-purification, enrichment, pre-fractionation and storage of peptides for proteomics using StageTips. *Nat. Protoc.* **2**, 1896–1906 (2007).
 92. A. A. Vinogradov, Z. P. Gates, C. Zhang, A. J. Quartararo, K. H. Halloran, B. L. Pentelute, Library design-facilitated high-throughput sequencing of synthetic peptide libraries. *ACS Comb. Sci.* **19**, 694–701 (2017).
 93. M. D. Simon, Y. Maki, A. A. Vinogradov, C. Zhang, H. Yu, Y.-S. Lin, Y. Kajihara, B. L. Pentelute, D-amino acid scan of two small proteins. *J. Am. Chem. Soc.* **138**, 12099–12111 (2016).
 94. T. L. Peeters, M. J. Macielag, I. Depoortere, Z. D. Konteatis, J. R. Florance, R. A. Lessor, A. Galdes, D-amino acid and alanine scans of the bioactive portion of porcine motilin. *Peptides* **13**, 1103–1107 (1992).
 95. F. Touti, Z. P. Gates, A. Bandyopdhyay, G. Lautrette, In-solution enrichment identifies peptide inhibitors of protein–protein interactions protein-protein interactions. *Nat. Chem. Biol.* **15**, 318–339 (2019).
 96. X. Ye, Y. C. Lee, Z. P. Gates, Y. Ling, J. C. Mortensen, F. S. Yang, Y. S. Lin, B. L. Pentelute, Binary combinatorial scanning reveals potent poly-alanine-substituted inhibitors of protein-protein interactions. *Commun. Chem.* **5**, 1–10 (2022).
 97. R. L. A. Dias, R. Fasan, K. Moehle, A. Renard, D. Obrecht, J. A. Robinson, Protein ligand design: From phage display to synthetic protein epitope mimetics in human antibody Fc-binding peptidomimetics. *J. Am. Chem. Soc.* **128**, 2726–2732 (2006).
 98. C. M. B. K. Kourra, N. Cramer, Converting disulfide bridges in native peptides to stable methylene thioacetals. *Chem. Sci.* **7**, 7007–7012 (2016).
 99. N. Hartrampf, A. Saebi, M. Poskus, Z. P. Gates, A. J. Callahan, A. E. Cowfer, S. Hanna, S. Antilla, C. K. Schissel, A. J. Quartararo, X. Ye, A. J. Mijalis, M. D. Simon, A. Loas, C. Jessen, T. E. Nielsen, B. L. Pentelute, Synthesis of proteins by automated flow chemistry. *Science* **368**, 980–987 (2020).
 100. A. J. Mijalis, D. A. Thomas, M. D. Simon, A. Adamo, R. Beaumont, K. F. Jensen, B. L. Pentelute, A fully automated flow-based approach for accelerated peptide synthesis. *Nat. Chem. Biol.* **13**, 464–466 (2017).

Acknowledgments: We thank A. J. Quartararo, A. Shimada, T. M. Wood, S. A. Antilla, and A. E. Cowfer for advice and suggestions on the methods developed here. We thank T. E. Nielsen and U. Stolz for helpful discussion in support of our work. **Funding:** Support for this work was provided by Novo Nordisk A/S. J.S.B. acknowledges support from Pharmaceutical Research and Manufacturers of America (PhRMA) Foundation through the Postdoctoral Fellowship in Drug Discovery. M.A.L. acknowledges support from the MIT Dean of Science Fellowship. **Author contributions:** Conceptualization: M.A.L., J.S.B., and B.L.P. Methodology: M.A.L. and J.S.B. Investigation: M.A.L., J.S.B., and C.E.F. Visualization: M.A.L. and J.S.B. Supervision: A.L. and B.L.P. Writing—original draft: M.A.L. and J.S.B. Writing—review and editing: M.A.L., J.S.B., C.E.F., A.L., and B.L.P. **Competing interests:** The authors declare the following competing interests: B.L.P. is a cofounder of Amide Technologies, Decoy Therapeutics, and New Frontier Bio, which are companies focusing on the development of protein and peptide therapeutics. The other authors declare that they have no competing interests. **Data and materials availability:** All data needed to evaluate the conclusions in the paper are present in the paper and/or the Supplementary Materials.

Submitted 14 June 2024
Accepted 11 February 2025
Published 19 March 2025
10.1126/sciadv.adr1018